Improvement of the Point Spread Function by Collimators' New Configuration in Nuclear Medicine

Mansour Ashoor
Nuclear Science and Technology Research Institute
Abdollah Khorshidi (abkhorshidi@yahoo.com)
Gerash University of Medical Sciences https://orcid.org/0000-0002-6674-8789

Research

Keywords: Collimator, Point Spread Function, Resolution, Nuclear Medicine, Monte Carlo method, MCNPX

Posted Date: June 11th, 2021

DOI: https://doi.org/10.21203/rs.3.rs-595223/v1

Improvement of the point spread function by collimators' new configuration in nuclear medicine

Mansour Ashoor [1], Abdollah Khorshidi [2*]

[1] Radiation Applications Research School, Nuclear Science and Technology Research Institute, P.O. Box: 113653486, Tehran, Iran.

[2] School of Paramedical, Gerash University of Medical Sciences, P.O. Box 7441758666, Gerash, Iran.

* Corresponding author's Email: abkhorshidi@yahoo.com

Tel: +989102104856

Fax: +987152447542

Short Running Title: PSF improvement in nuclear medicine by collimator configuration

Highlights

- New configuration of parallel collimators is presented as geometrical combination to improve PSF.
- By raising scattering γ rays, the PSF was converted from delta function to Gaussian distribution.
- By increasing energy, the PSF was more broadened because of more penetration strength.
- The CCS collimator led to better resolution compared to the PC one in detecting smaller lesions.

Summary

What is already known about this subject?

The Parallel Hole Collimators (PCs) are the most common case used in SPECT based on sensitivity and resolution. Here a novel geometric combination of conical, cylindrical and spherical (CCS) volumes is proposed to improve the full width at half maximum (FWHM) of the point spread function (PSF).

What are the new findings?

The simulation findings revealed that the PSF in the CCS configuration is narrower than that of the cylindrical one for all energies, in order to improve the resolution when differentiating smaller lesions.

How might it impact on clinical practice in the foreseeable future?

By optimizing the collimators used in nuclear medicine, unwanted gamma rays are eliminated and the signal-to-noise ratio is augmented.

ABSTRACT

Objective: The collimators in which the various geometrical configurations have been suggested to optimize the sensitivity and resolution have a key role in acquiring the qualified images in nuclear medicine towards a better recognition of some diseases.

Methods: In this study, a new configuration as a geometrical combination of the conical, cylindrical and spherical (CCS) volumes for parallel hole collimators which is assessed by using the volumetric-parametric method has been introduced to improve point spread function (PSF) being the collimators response on the radioactive point source. It has been simulated by the MCNPX code at the various energies values of the point source along with the traditional collimator in which included the cylindrical volume only.

Results: The PSF will transmogrify from a delta function to a distribution which can correlate with a Gaussian distribution, while the scattered gamma rays were increased. The simulation results have indicated that the PSF in the CCS configuration is narrower than that of the cylindrical one at all the energies, leading the improvement of the resolution. Also, the theoretical results are agreement with the simulated ones. The more the energy value of the source, the more broaden the PSF will be due the more penetration strength. The narrower the PSF, the better the qualified image will be.

Conclusion: This method may be employed to determine the accurate attenuation coefficient of absorbers as well.

Keywords: Collimator; Point Spread Function; Resolution; Nuclear Medicine; Monte Carlo method; MCNPX.

1. Introduction

The photons originating from the tissue should be rationally guided to the gamma camera by collimators along with attenuation of the scattered photons. The more the attenuation, the better qualified image will be. The well-managed gamma photons have involved in appraising the radiopharmaceutical concentration as a criterion for the uptake of radiotracers by a target organ as well as in the acquisition of functional and anatomical images in order to characterize the physiological parameters such as glomerular filtration rate (GFR), blood flow (BF) and so on. The image properties such as contrast, resolution, and signal to noise ratio (SNR) can be altered by varying the geometrical specifications of collimators [1].

In general, the collimators have eliminated well the unwanted gamma rays, and have affected the resolution as well as the number of counts detected [2]. Performance of parallel-hole collimators may be evaluated by determining their response to a radioactive point source which for instance, the amount of collimator resolution is calculated via measuring the full width at half maximum (FWHM) of point spread function (PSF). The accurate determination of the collimator PSF is requirement for quantitative analysis of SPECT data [3].

The parallel hole collimators (PCs) are the most common case used in SPECT. They have been categorized into different types established upon their sensitivity and resolution besides the photon energy derived from radiopharmaceutical. A general way to improve the sensitivity of PCs is to reduce the hole length and/or to raise the hole size. This method increases the space entry angle of holes, so that more gamma rays pass through the holes and the sensitivity is increased. The widening of the solid angle of the collimator holes, however, leads to a widening of the PSF and, accordingly, to a deterioration in the resolution. By increasing the sensitivity in the PCs, the PSF is increased in both width and height. Consequently, the FWHM value increases and the image resolution deteriorates. Much effort has been executed to raise the PCs sensitivity without deteriorating the resolution, or vice versa, via representing novel plans and optimizing the geometric configurations of collimator [4-10]. One of the most significant difficulties collaborated with the PCs is compromise between sensitivity and resolution [11] that this problem has been roughly solved by extended parallel hole collimators (EPCs). Increasing the sensitivity of EPCs increases the height of the PSF more than the width. In other words, unlike the PCs, the deterioration in resolution could be limited by increasing the sensitivity in EPCs [12]. In addition, calculation algorithms have been proposed to balance this deterioration caused by the highly sensitive collimator [13]. We have introduced an optimized computational method to improve the PCs' response in nuclear medicine before the response can be obtained with a higher accuracy [14]. This is an alternative technique to enhance this compromise. Although this compromise has been improved on the converging collimators like cone beam and fan beam, the field of view (FOV) is limited. By converging collimators, lessening the distance from the object to the focal point increases the magnification of acquired image; reciprocally, a smaller fraction of the object is shown [15-20].

In this research, we have proposed a novel geometrical plan on the PCs, namely the conical, cylindrical and spherical (CCS) collimator to narrow the PSF, leading the better resolution. An appropriate theory is introduced using the volumetric-parametric technique, and Monte Carlo simulations using the MCNPX code have been carried out to investigate and compare the CCS and PC collimators.

2. Materials and Methods

2.1. Theory

At first, we look at the delta function briefly. The delta function can be viewed as the approach of a square pulse with the pulse width (a) moves toward zero, which the pulse height will move toward infinity. Let this pulse be defined as;

$$\delta_{pluse}(x) = \begin{cases} \frac{1}{a}, & -\frac{a}{2} \leq x \leq \frac{a}{2} \\ 0, & otherwise \end{cases} \qquad (1)$$

Apparently, the smaller parameter of a results in a narrower and higher the pulse. The integral over the pulse will always be 1 as well. Eq. (2) indicates the Fourier series of the delta function.

$$\delta_{Fourier}(x) = \frac{1}{2a} + \sum_{n=1}^{n_{max}} \frac{1}{a} \cos\left(n \frac{[\pi]}{a} x\right) \qquad (2)$$

Fig. 1 demonstrates the expanded Fourier series for this function. The peak is more pronounced due to the higher order in the expansion.

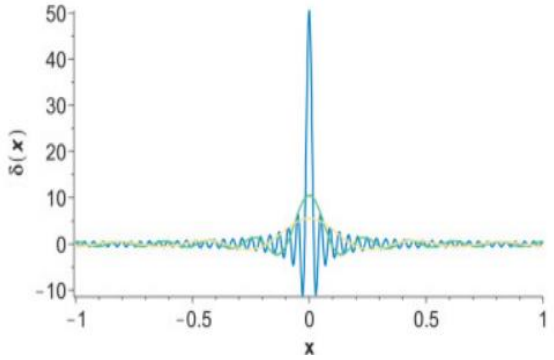

Fig. 1. The expanded Fourier series for delta function, $\delta_{Fourier}(x)$.

Also, the Fourier integral representation of the delta function is as follows;

$$\delta(t) = \frac{1}{2\pi} \int_{-\infty}^{\infty} e^{i\omega t} d\omega \qquad (3)$$

The PSF should be ideally as the delta function, but it will transmogrify from a delta function to a distribution which can correlate with a Gaussian distribution, while the scattered gamma rays were increased. The Gaussian function, g(x), is defined as,

$$g(x) = \frac{1}{\sigma\sqrt{2\pi}} e^{\frac{-x^2}{2\sigma^2}} \qquad (4)$$

where it is normalized to 1 as:

$$\int_{-\infty}^{\infty} g(x)dx = 1$$

The Fourier transform of the Gaussian function is as follow:

$$G(\omega) = e^{-\frac{\omega^2\sigma^2}{2}} \qquad (5)$$

The σ parameter is an index to characterize the resolution. The lower the σ parameter, the better the resolution will be. Generally, collimators are able to decrease the scattered gamma rays as well as have the various configurations to reach the specific targets. The resolution and sensitivity parameters on the collimators act against. Thus, there is a tradeoff between them. To solve this problem, one may focus on the geometry specifications of collimators. In this survey, a novel design, conical, cylindrical and spherical (CCS) is characterized in which conical denticles are annexed to the collimator septa on the detector side and spherical denticles are annexed below the collimator septa on the source side, has been suggested to enhance the performance of the PCs. In other words, the PC has been modified as the conical, cylindrical and spherical which is assessed by using the volumetric-parametric method, as shown in Fig. 2. Assuming $l = \alpha \times h$, the volumetric ratio of the CCS collimator to the PC one will be as follows;

$$\frac{V_{CCS}}{V_{pc}} = 1 + \frac{1}{3}\alpha + \frac{2}{3}\left(\frac{r}{h}\right) \qquad (6)$$

Where l, r, and h are the height of the conic, cylinder radius, and the sphere radius, correspondingly. The α parameter is a constant value. The volumetric ratio is a basic criterion here because shows the rate of the improving the PSF as well.

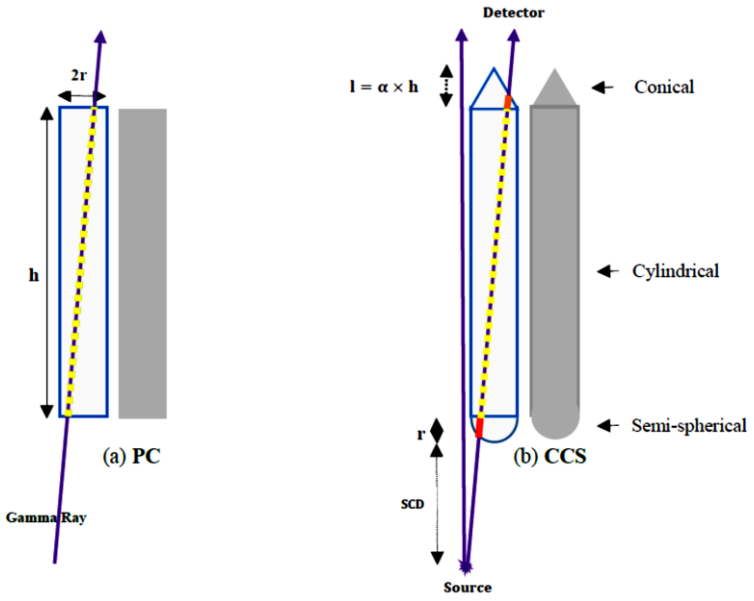

Fig. 2. Schematic of the collimators configurations; (**a**) the parallel hole (PC), and (**b**) the conical, cylindrical and spherical (CCS). The *SCD* parameter is the source-collimator distance.

The changes of collimator volumetric ratio against the changes of the height and radius of cylinder at the various amounts of the α parameter (0.01, 0.0526, and 0.1) have been calculated by the MATLAB

software, as shown in Fig. 3. The volumetric ratio is increased with increasing the α parameter. In other words, the volumetric ratio is increased by increase the conical height.

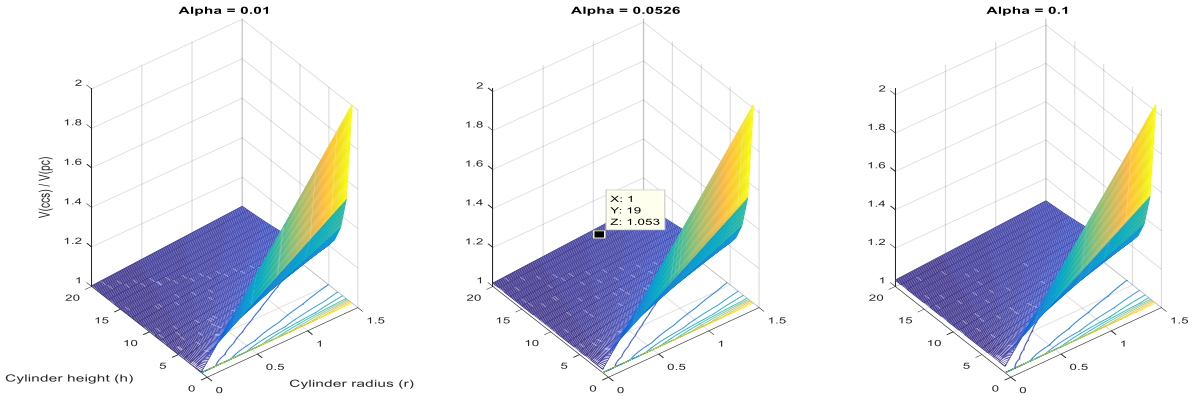

Fig. 3. The changes of collimator volumetric ratio via the changes of the height and radius of cylinder at the various amounts of the $\boldsymbol{\alpha}$ parameter (0.01, 0.0526, and 0.1). In simulations, the α parameter, cylinder height and radius are 0.0526, 19 and 1, correspondingly (black square marker).

The α parameter, cylinder height and radius are 0.0526, 19 and 1, correspondingly for simulations performing by the MCNPX code as well as the linear changes of collimator volumetric ratio via the changes of α parameter at cylinder height of 19 mm and radius of 1 mm have been shown in Fig. 4.

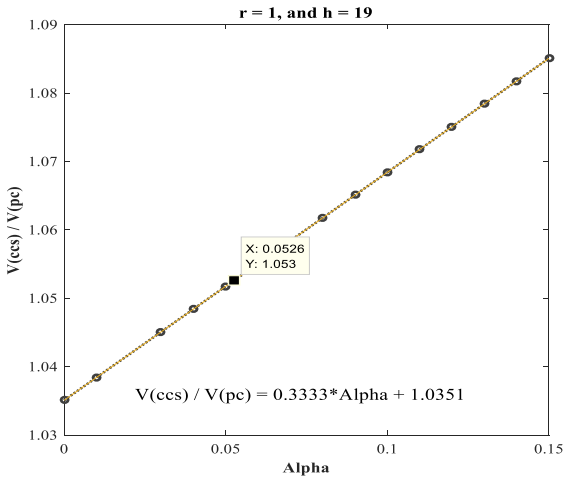

Fig. 4. The linear changes of collimator volumetric ratio via the changes of the **α** parameter at r = 1, and h = 19 mm.

Also, the tracks of the ray in the collimators indicated in Fig. 2 are calculated. The changes of collimator tracks ratio value against the changes of the cylinder height and the conic height at the r = 1, d = 3, and SCD = 1 mm have been calculated by the MATLAB software, as shown in Fig. 5. The tracks ratio is increased with decreasing the *h* parameter as well as *l* one. However, the tracks ratio is always more than one. The more this ratio, the better resolution and the lower the σ will be.

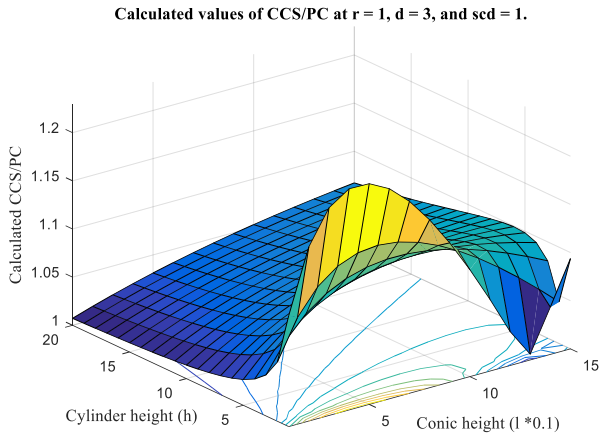

Fig. 5. The changes of collimator tracks ratio value against the changes of the cylinder height and the conic height at the r = 1, d = 3, and SCD = 1 mm.

2.2. Monte Carlo Simulation by MCNPX code

The interactions of radiation with materials are different due to the variety of media of energy and matter, in which the density plays a key role. These interactions and complex transports were modeled by the Monte Carlo method [21]. In this research, the Monte Carlo N-Particles code version X (MCNPX) was used which is applicable for the approachability and rule of extensive parameters included in the calculations, whereby a history of the contribution of each photon is obtained. The code enables the tractable recognition of the particles established upon the cross-sections of various interactions. The examination of the energy transfer was carried out by settling the characteristics of the cross-section of an interaction, since the scattering and absorption cross-sections of the simulations from the ENDF/B-VII.1 libraries were taken into account [22]. The deformation of the geometric shape changes the cross sectional area. In general, three assessors for flux are as surface intersection (F2), track-length (F4) and next-event (ring and point detectors). These are appraisal of the amount

$$\iint_{t,E} \emptyset(\mathbf{r}, \mathrm{E}, \mathrm{t})\mathrm{dEdt} \qquad (7)$$

The integral is over time and energy, causing to units of particles per cm^2. The integration range can be scrutinized by the T and E cards. The flux time units are examined by the units of the source; that is *tally* depict fluence tally when the source has unit of particles per unit time. In simulations, the track length assessor (F4) is selected here, which utilizes the basic explanation of fluence as the number of particle-trajectory lengths per unit volume.

The PCs and CCS configurations are simulated by the MCNPX code and compared using the FWHM quantities. These configurations with a hole size of 2 mm and hole length of 19 mm, and the α of 1/19 are considered for assessment of the performance of CCS', as shown in Table 1. The energy amounts

of radioactive point sources were 50, 140, 510, 1710 keV. Each simulation involved the emission of 10^8 photons to produce the PSF.

Table 1. The geometrical characteristics of the collimators configurations (in mm).

Collimator	**PC**	**CCS**
Cylinder radius (**r**)	1	1
Cylinder height (**h**)	19	19
Conic height (**l**)	-	1
α parameter	-	0.0526

The model comprises of a point source below the collimator and a simple point detector above the collimator, which discovers all gamma photons that hit it. The point detector is placed within collimator holes at above. A gamma photon emitted by the source enters the designed collimator, passes through division of collimator septa, leaves the collimator through the floor, and eventually may be mapped via the scintillation camera at designated point [23]. The probability that such a gamma photon essentially reaches the image plane is resolved via the distance passed by the collimator septa and the attenuation coefficient of the collimator material. For simplicity at the comparison, the collimators are placed in one row with the BF_3 material. In order to rationalize directional dependence of the passage of photons through the designed holes in Fig. 1, the point sources were placed at the 1-mm source-collimator distance on the central axis of the major holes of the CCS and PC. The count profile for the major holes along the Y axis from one wall apex through the opposite wall was estimated applying the F4 tally in point detector cells with the size of 0.4 mm within the cylinders. By tracking a beam through the collimator and determining the distance passed in the septa, the radiation flux through the detector is decided. The PSF is established by repetition procedure for 10^8 beams, discretized by the angle of emission at the designated point source.

3. Results

The simulated results of the PC and CCS configurations by the MCNPX code have been indicated in Fig. 6.

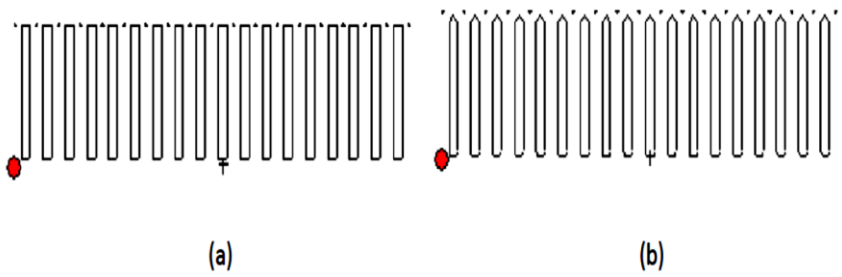

Fig. 6. The simulated geometrical results of the configurations by the MCNPX code; (**a**) the PC, and (**b**) CCS collimator. The radioactive point sources have been indicated by the red-circle markers, and the point detector is the other side where the F4 tally is calculated.

The F4 tally is calculated to determine the PSF at the various energies of the source for the PC and CCS collimators. The PSF curve for the CCS collimator is narrower than that of the PC one, leading the better resolution, as shown in Fig. 7.

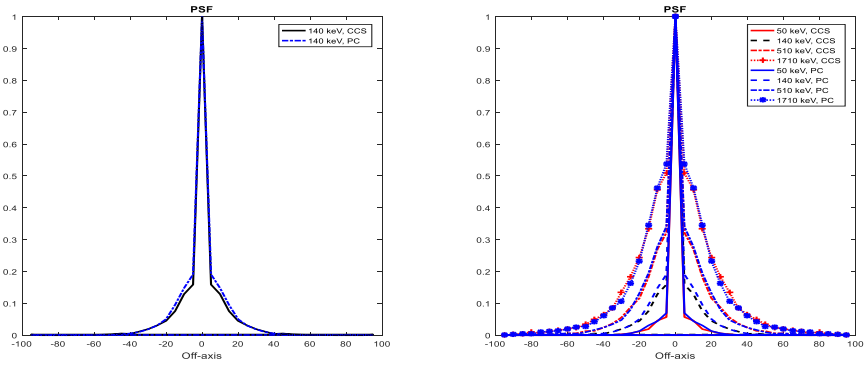

Fig. 7. The simulated PSF at the different energies of the source for the PC and CCS collimators.

On the other hand, the mean amounts of the PSF are the same the theoretical results obtained from the volumetric method at the various energies of the source. At the 140-keV point source, the relative error between the simulated and theoretical results is minimum (0.29%), and at the 1710-keV is maximum (5.73%), as shown in Table 2 and Fig. 8.

Table 2. The simulated mean PSF and theoretical (V_{ccs}/V_{pc}) results at the various energies along with their relative errors.

E (keV)	**50**	**140**	**510**	**1710**
Theory (V_{ccs}/V_{pc})	0.95	0.95	0.95	0.95
Simulated mean PSF	0.98	0.95	0.98	1.01
Relative error %	2.95	0.29	3.13	5.73

As known, the interactions are based on the photoelectric and Compton processes. The photoelectric coefficient diminishes by raising energy at low energies and is negligible for the simulated energy of 1710 keV. In contrast, the Compton coefficient is reduced by raising energy at low energies, but after a critical energy amount is reached the coefficient becomes constant by raising energy before it decreases sharply above a second critical amount. The Compton coefficient is roughly constant at energies of 1710 keV.

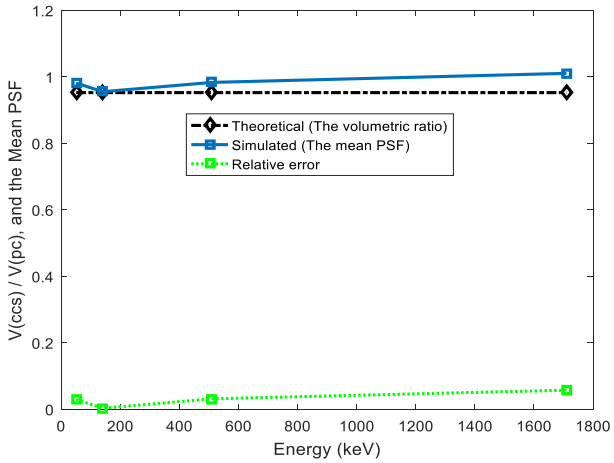

Fig. 8. The simulated mean amounts of the PSF and the theoretical-volumetric results via the energy values along with the relative error.

Fig. 9 and Table 3 show the amounts of the **σ** parameter indicating a criterion for FWHM at the various energies of the source for the PC and CCS collimators.

Table 3. The amounts of the σ parameter for the PC and CCS collimators at the various energies of the point source.

	50pc	**50ccs**	**140pc**	**140ccs**	**510pc**	**510ccs**	**1710pc**	**1710ccs**
σ	0.4268	0.4242	0.4938	0.4740	0.5975	0.5842	0.9108	0.8393

The CCS collimator has the **σ** value lower than that of the PC one at all the energies, resulting a better resolution.

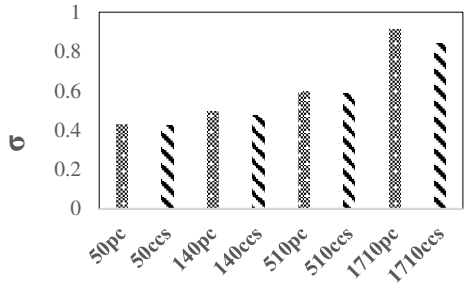

Fig. 9. The amounts of the σ parameter for the CCS and PC collimators at the various energies of the source.

The relationship between the amounts of the σ parameter in $\times 10^{-4}$ mm at the various energies of the source in keV has been formulated as the $\sigma_{PC} = 3E + 4392$ and $\sigma_{CCS} = 2E + 4355$ for the PC and CCS collimators, respectively as shown in Fig. 10. The σ parameter at the CCS collimator is lower than that of the PC one at all the energies. In other words, the CCs resolution is better than that of the PC.

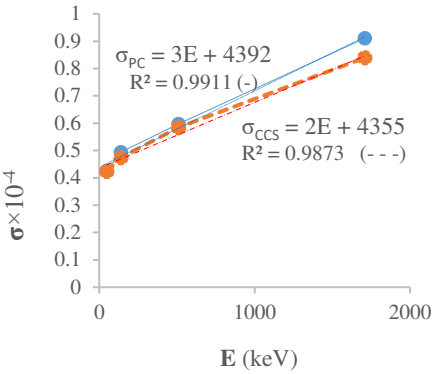

Fig. 10. The amounts of the σ parameter in $\times 10^{-4}$ mm at the various energies for the CCS and PC collimators.

4. Discussion

One potential benefit of nuclear medicine is the ability to infer quantitative information like the amount of radio-labeled tracer that is taken up by tumor or particular organ. The collimators can get the qualified images for metabolic performance and enhanced diagnosis of the lesions. With the collimators utilized in nuclear medicine merely about one in ten thousand of the emitted photons travel through the collimator. Therefore, the collimator design necessitates detailed knowledge of the relationship between the collimator geometry and the resulting imaging properties and has an important impact on the comprehensive performance of the gamma camera by virtue of the restriction on the number of counts captured. Although novel plans and optimized ways besides analytical pattern have been suggested to progress the compromise between sensitivity and resolution in the collimators, the conflicting procedure of these collimators still stays one of the main issues correlated with the PCs. In this survey, the CCS collimator was proposed in which conical denticles were placed on the collimator septa on the detector side and spherical denticles were placed below the collimator septa on the source side to enhance the PCs performance.

In order to optimize a collimator design for quantification, the Monte Carlo calculation can be examined using the interactions of beams in the materials, on the basis of scattering and absorption cross-sections resulting from the Compton and photoelectric procedures that enable the fluence may be estimated [24-26]. The contribution of the photoelectric and Compton coefficients at different energies was different from each other. Generally, at a distinct energy amount, the Compton procedure tends to dominate the photoelectric procedures, which implies that the number of scattered photons is raised [2]. The conical denticles upon the CCS may reduce the number of scattered photons, as shown in Fig. 7. This of course depends on the energy value of the radioactive point source.

In SPECT, the image produced by a point source is deteriorated by a number of factors associated with detectors and collimators such as geometric response, intrinsic response, septal scattering, and septal penetration. The geometric response is because of the collimator dimensions and the geometric

response function gets to be broader as the distance from the collimator face increases and is highly dependent on the particular design of each collimator. However, the obtained images are blurred by the intrinsic system PSF, so that a finite spatial resolution worsens the contrast of subject lesions [27]. The total resolution results from the convolution of the collimator PSF with the PSF of the intrinsic gamma camera. The intrinsic PSF is typically well approached radially by a symmetric Gaussian function. The spatial resolution of the collimator deteriorates linearly with raising distance from the collimator surface. Moreover, the level of image noise affects the accuracy with which activity can be evaluated, suggesting that collimators with high efficiency are desirable. The CCS has indicated to improve the resolution compared to the PC.

The diagnostic tasks that must be executed with SPECT imaging of the brain require the location and identification of ganglional and cortical structures, as well as the detection of lesions in size, form, or uptake [28,29]. Hanson found that optimal performance for localization, sizing, and object separation requires more high spatial frequency information than for detection, even with a uniform background. He also showed that an uneven background reduces the importance of information with low spatial frequency [30]. These estimations are supported by a simulation survey recently conducted by Muehllehner, which shows that the counts number obtained for a given SNR reduces by raising resolution for higher-order tasks such as separating high-contrast rods or bars [31]. The loss of resolution by virtue of the presence of high-energy gamma photons was less for the CCS than for the PC.

A higher resolution system can transmit more high frequency data. This enhances the image contrast and becomes more and more important for lesion recognition as the tumor size reduces. When higher-order attempts like locating and identifying ganglional and cortical structures and detecting lesions with various form and uptake are considered, the augmented resolution outweighs the loss of sensitivity. Therefore, collimators should be designed in such a way that they offer elevated resolution, even at the cost of sensitivity. To improve the cost function, one may optimize the geometric parameters of the CCS using the genetic algorithm [32], which is outside the aim of this survey.

The only restrictions placed on the dimensions are due to: (1) weight restrictions (2) the minimum septa thickness imposed by manufacturing restrictions (3) the visibility of the collimator hole model in the obtained images. Meanwhile, some restrictions on geometrical symmetry are enforced in order to uphold the spatial invariance of the PSF [33]. Besides, the other imaging systems such as MRI can record the organs of the body in detailed, which can help augment the medical information in combination with nuclear medicine [34-37].

5. Conclusion

Optimization of the collimator configurations towards the better resolution and SNR is one of the most aims in nuclear medicine. The uncertainty about the origin of the discovered gamma photons is

investigated by a point spread function. The proposed CCS collimator is able to improve the PSF, leading the better resolution compared to the PC one. This collimator may be useful to map the smaller lesions and tumors.

Declarations

• List of abbreviations

PC: Parallel hole collimator

CCS: Conical, cylindrical and spherical

FWHM: Full width at half maximum

PSF: Point spread function

GFR: Glomerular filtration rate

BF: Blood flow

SNR: Signal to noise ratio

EPC: Extended parallel hole collimator

FOV: Field of view

MCNPX: Monte Carlo N-Particles code version X

• Ethics approval and consent to participate: Not applicable

• Consent to publish: Not applicable

• Availability of data and materials: All data required to support the results and conclusions of the study have been provided here with the submission.

• Competing interests: Not applicable

• Funding: Not applicable

• Authors' Contributions

Abdollah Khorshidi: Conceptualization, Data curation, Formal analysis, Investigation, Methodology, Software, Supervision, Validation, Visualization, Writing – original draft.

Mansour Ashoor: Data curation, Investigation, Formal analysis, Software, Validation.

• Acknowledgements: Not applicable

References

[1] Lee Y, Ryu HJ, Lee SW, Park SJ, Kim HJ. Comparison of ultra-high-resolution parallel-hole collimator materials based on the CdTe pixelated semiconductor SPECT system. Nucl. Instrum. Methods. A 2013; 713: 33-39.

[2] Fuin N, Bousse A, Pedemonte S, Arridge S, Ourselin S, Hutton B. Collimator design in SPECT, an optimisation tool. IEEE Nuclear Science Symposuim & Medical Imaging Conference, 2010.

[3] Ashoor M, Asgari A, Khorshidi A, Rezaei A. Evaluation of Compton attenuation and photoelectric absorption coefficients by convolution of scattering and primary functions and counts ratio on energy spectra. Indian J. Nucl. Med. 2015; 30 (3): 239-247.

[4] Moslemi V, Ashoor M. Design and performance evaluation of a new high energy parallel hole collimator for radioiodine imaging by gamma cameras: Monte Carlo simulation study. Ann. Nucl. Med. 2017; 31 (4): 324-334.

[5] Lee YJ, Park SJ, Kim DH, Kim HJ. Optimization of the SPECT systems based on a CdTe pixelated semiconductor detector using novel parallel-hole collimators. J. Instrum. 2014; 9: C05057.

[6] Asgari A, Ashoor A, Sohrabpour M, Shokrani P, Rezaei A. Evaluation of various energy windows at different radionuclides for scatter and attenuation correction in nuclear medicine. Ann. Nucl. Med. 2015; 29: 375-383.

[7] Lowe D, Truman A, Kwok H, Bergman A. Optimization of the design of round-hole parallel collimators for ultra-compact nuclear medicine imaging. Nucl. Instrum. Methods. A. 2002; 621: 406-412.

[8] Giokaris N, Loudos G, Maintas D, Karabarbounis A, Spanoudaki V, Stiliaris E, Boukis S, Gektin A, Boyarintsev A, Pedash V, Gayshan V. Crystal and collimator optimization studies of a high-resolution γ-camera based on a position sensitive photomultiplier. Nucl. Instrum. Methods. A 2004; 527: 134-142.

[9] Khorshidi A. Accelerator driven neutron source design via beryllium target and 208Pb moderator for boron neutron capture therapy in alternative treatment strategy by Monte Carlo method. J Can Res Ther 2017; 13: 456-65.

[10] Ghaly M, Links JM, Frey EC. Collimator optimization and collimator-detector response compensation in myocardial perfusion SPECT using the ideal observer with and without model mismatch and an anthropomorphic model observer. Phys. Med. Biol. 2016; 61: 2048-2066.

[11] Asmaand E, Manjeshwar R. Evaluation of the impact of resolution-sensitivity tradeoffs on detection performance for SPECT imaging. IEEE. Nucl. Sci. Symp. 2008; 3730-3733.

[12] Moslemi V, Ashoor M. Introducing a Novel Parallel Hole Collimator: The Theoretical and Monte Carlo Investigations, IEEE. Trans. Nucl. Sci. 2017; 64 (9): 2578-2587.

[13] Zhang B, Zeng GL. High-resolution versus high-sensitivity SPECT imaging with geometric blurring compensation for various parallel-hole collimation geometries. IEEE Trans. Inf. Technol. Biomed. 2010; 14: 1121-1127.

[14] Moslemi V, Ashoor M. Introducing an Optimized Computing Method to Improve Parallel-Hole Collimators' Response in Nuclear Medicine. J. of Nucl. Sci. and Tech. 2019; 87 (2): 26-36.

[15] Watanabe K, Sugiyama J, Yamazaki A, Uritani A. Development of a gamma-camera with a functional collimator. Nucl. Instrum. Methods. A. 2011; 652: 582-586.

[16] Tsui BMW, Lewis DP, Li J. Detection efficiencies of parallel, fan and cone beam collimators for source distributions in an attenuating medium. IEEE Nucl. Sci. Symp. 1999; 3: 1145-1149.

[17] Khorshidi A, Ashoor M, Hosseini SH, Rajaee A. Estimation of fan beam and parallel beam parameters in a wire mesh design. J. Nucl. Med. Tech. 2012; 40: 37-43.

[18] Khorshidi A, Ashoor M. Modulation transfer function assessment in parallel beam and fan beam collimators with square and cylindrical holes. Ann. Nucl. Med. 2014; 28: 363-370.

[19] Khorshidi A, Ashoor M, Hosseini SH, Rajaee A. Evaluation of collimators' response: Round and hexagonal holes in parallel and fan beam. Prog. Biophys. Mol. Bio. 2012; 109: 59-66.

[20] Ahmed ASMS, Kramer GH, Semmler W, Peter J. Performance study of a fan beam collimator designed for a multi-modality small animal imaging device. Nucl. Instrum. Methods. A. 2011; 629 (1): 368-376.

[21] Hughes HG et al. MCNPX™ 2.4.0, user's manual, version 2.4.0, LA-CP-02-408. Los Alamos National Laboratory, 2002.

[22] ENDF/B-VII.1. US Evaluated Nuclear Data Library. 2011. https ://www-nds.iaea.org/exfor /endf.htm. Accessed 2 Sept 2015.

[23] Han G, Z Liang Z, You J. A fast ray-tracing technique for tct and ect studies. Proc. IEEE Nucl. Sci. Symp. 1999.

[24] Asgari A, Ashoor M, Sarkhosh L, Khorshidi A, Shokrani P. Determination of Gamma Camera's Calibration Factors for Quantitation of Diagnostic Radionuclides in Simultaneous Scattering and Attenuation Correction. Current Radiopharmaceuticals 2019; 12 (1): 29-39.

[25] Ashoor M, Khorshidi A. Evaluation of Crystals' Morphology on Detection Efficiency Using Modern Classification Criterion and Monte Carlo Method in Nuclear Medicine. Proc. Natl. Acad. Sci., India, Sect. A Phys. Sci. 2019; 89: 579–585.

[26] Nabipour JS, Khorshidi A. Spectroscopy and Optimizing Semiconductor Detector Data Under X and γ Photons Using Image Processing Technique. Journal of Medical Imaging and Radiation Sciences 2018; 49 (2): 194-200.

[27] Moore KKSC, Cullum I. Collimator design for single photon emission tomography. Eur. J. Nucl. Med. 1992; 19: 138-150.

[28] Mueller SP, Polak JF, Kijewski MF, Holman BL. Collimator Selection for SPECT Brain Imaging: The Advantage of High Resolution. J. Nucl. Med. 1986; 27: 1729-1738.

[29] Khorshidi A. Assessment of SPECT images using UHRFB and other low-energy collimators in brain study by Hoffman phantom and manufactured defects. Eur. Phys. J. Plus 2020; 135:261.

[30] Hanson KM. Variations in task and the ideal observer. Proc SPIE 1983; 419: 60-67.

[31] Muehllehner G. Effect of resolution improvement on required count density in ECT imaging: A computed simulation. Phys Med Biol 1985; 30: 163-173.

[32] Rabiei M, Khorshidi A, Soltani-Nabipour J. Production of Yttrium-86 radioisotope using genetic algorithm and neural network. Biomedical Signal Processing and Control 2021; 66: 102449.

[33] Wernick MN, Aarsvold JN. Emission Tomography. Elsevier Academi Press, 2004.

[34] Ashoor M, Khorshidi A. Estimation of the Number of Compartments Associated With the Apparent Diffusion Coefficient in MRI: The Theoretical and Experimental Investigations. American J. Roentgeno. 2016; 206: 455-462.

[35] Ashoor M, Khorshidi A, Sarkhosh L. Estimation of microvascular capillary physical parameters using MRI assuming a pseudo liquid drop as model of fluid exchange on the cellular level. Reports of Practical Oncology & Radiotherapy 2019; 24 (1): 3-11.

[36] Ashoor M, Khorshidi A, Pirouzi A, Abdollahi A, Mohsenzadeh M, Barzi SMZ. Estimation of Reynolds number on microvasculature capillary bed using diffusion and perfusion MRI: the theoretical and experimental investigations. Eur. Phys. J. Plus 2021; 136: 152.

[37] Khorshidi A. Radiochemical parameters of molybdenum-99 transmutation in cyclotron-based production method using a neutron activator design for nuclear-medicine aims. Eur. Phys. J. Plus 2019; 134: 249

Figures

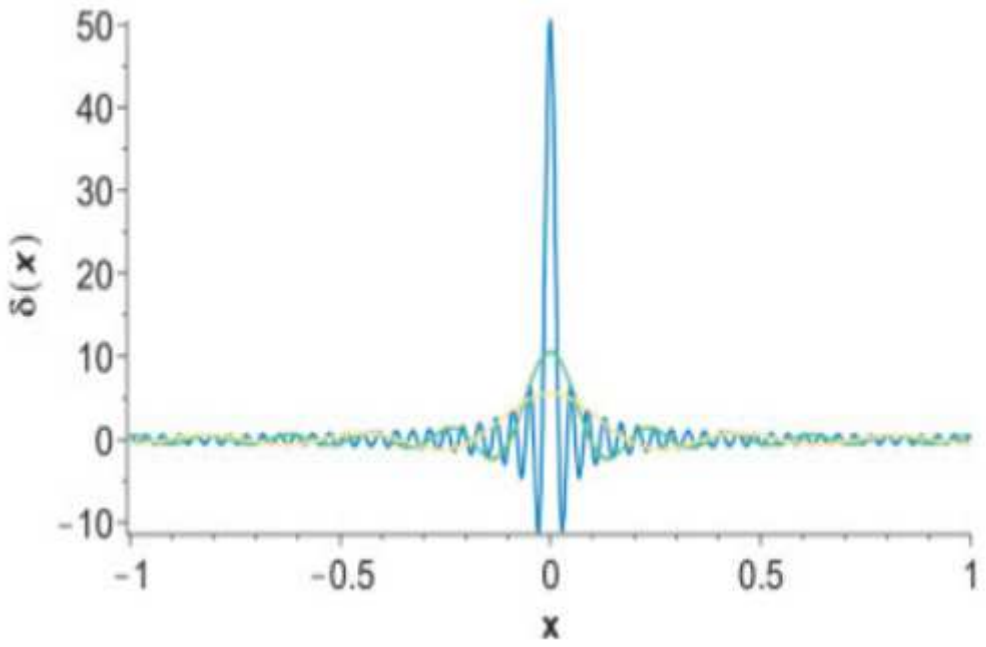

Figure 1

The expanded Fourier series for delta function, δFourier (x).

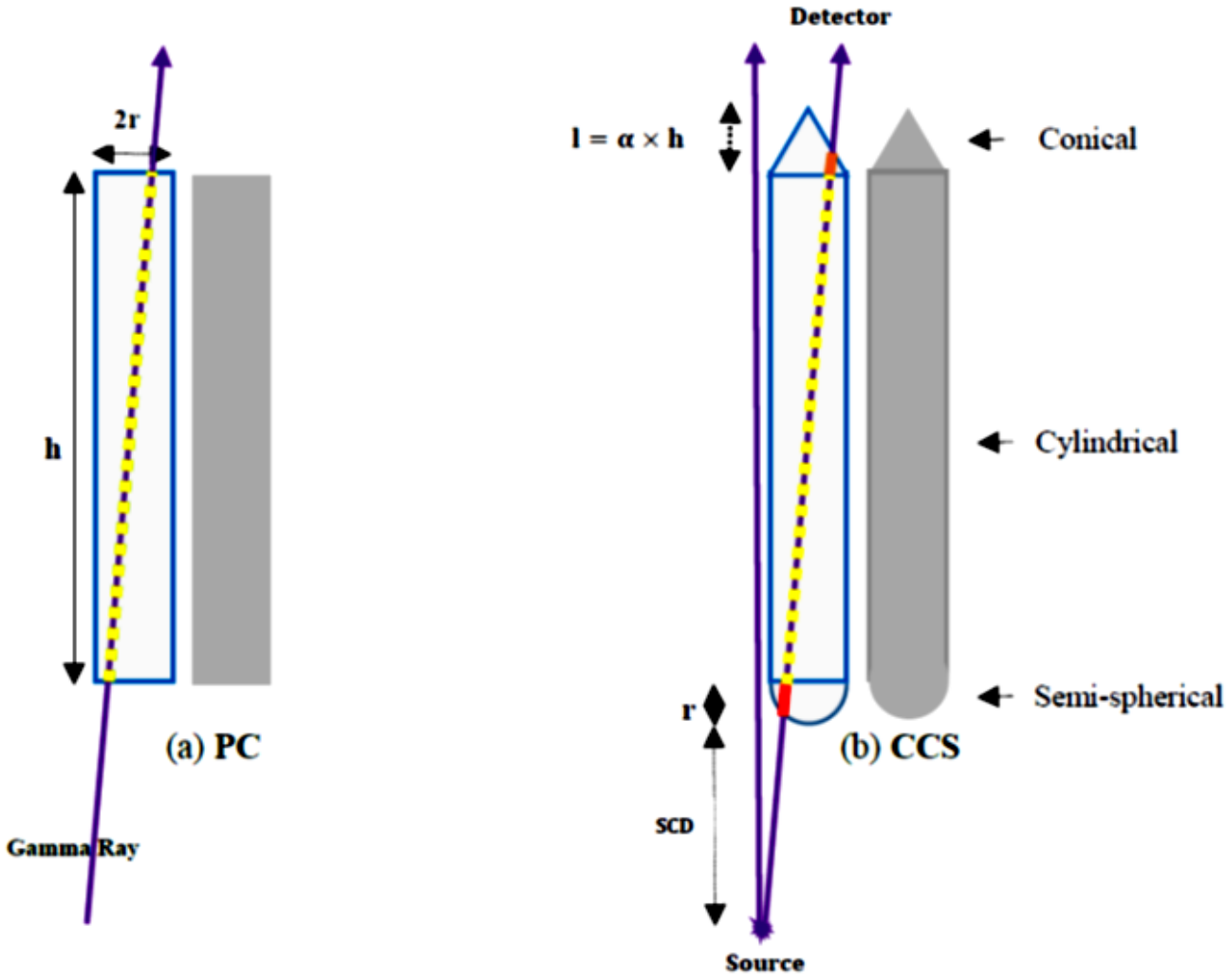

Figure 2

Schematic of the collimators configurations; (a) the parallel hole (PC), and (b) the conical, cylindrical and spherical (CCS). The SCD parameter is the source-collimator distance.

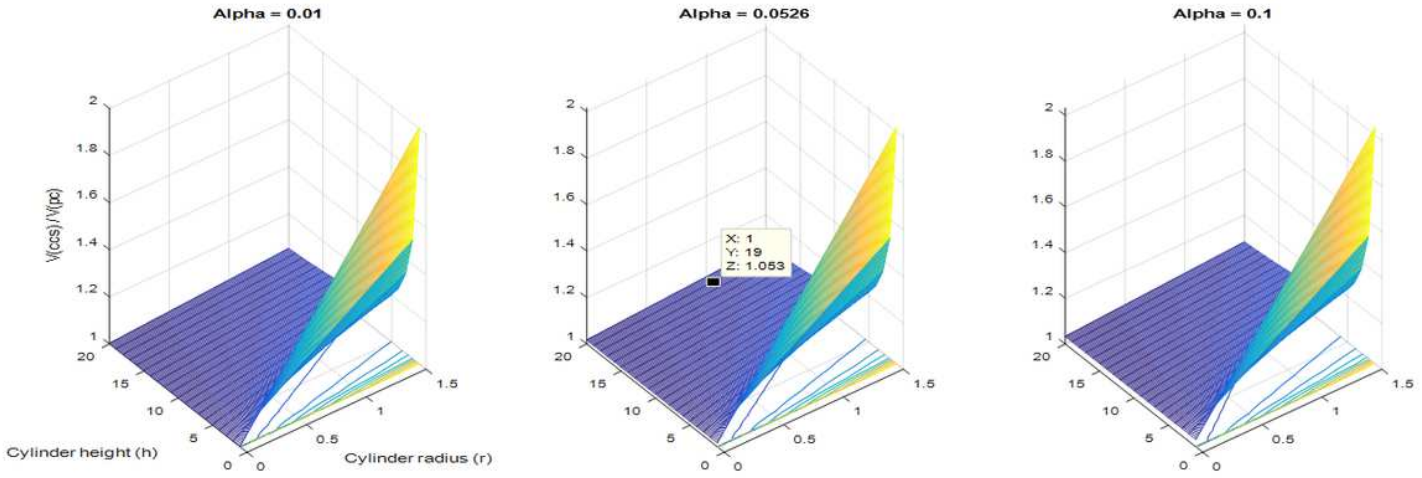

Figure 3

The changes of collimator volumetric ratio via the changes of the height and radius of cylinder at the various amounts of the α parameter (0.01, 0.0526, and 0.1). In simulations, the α parameter, cylinder height and radius are 0.0526, 19 and 1, correspondingly (black square marker).

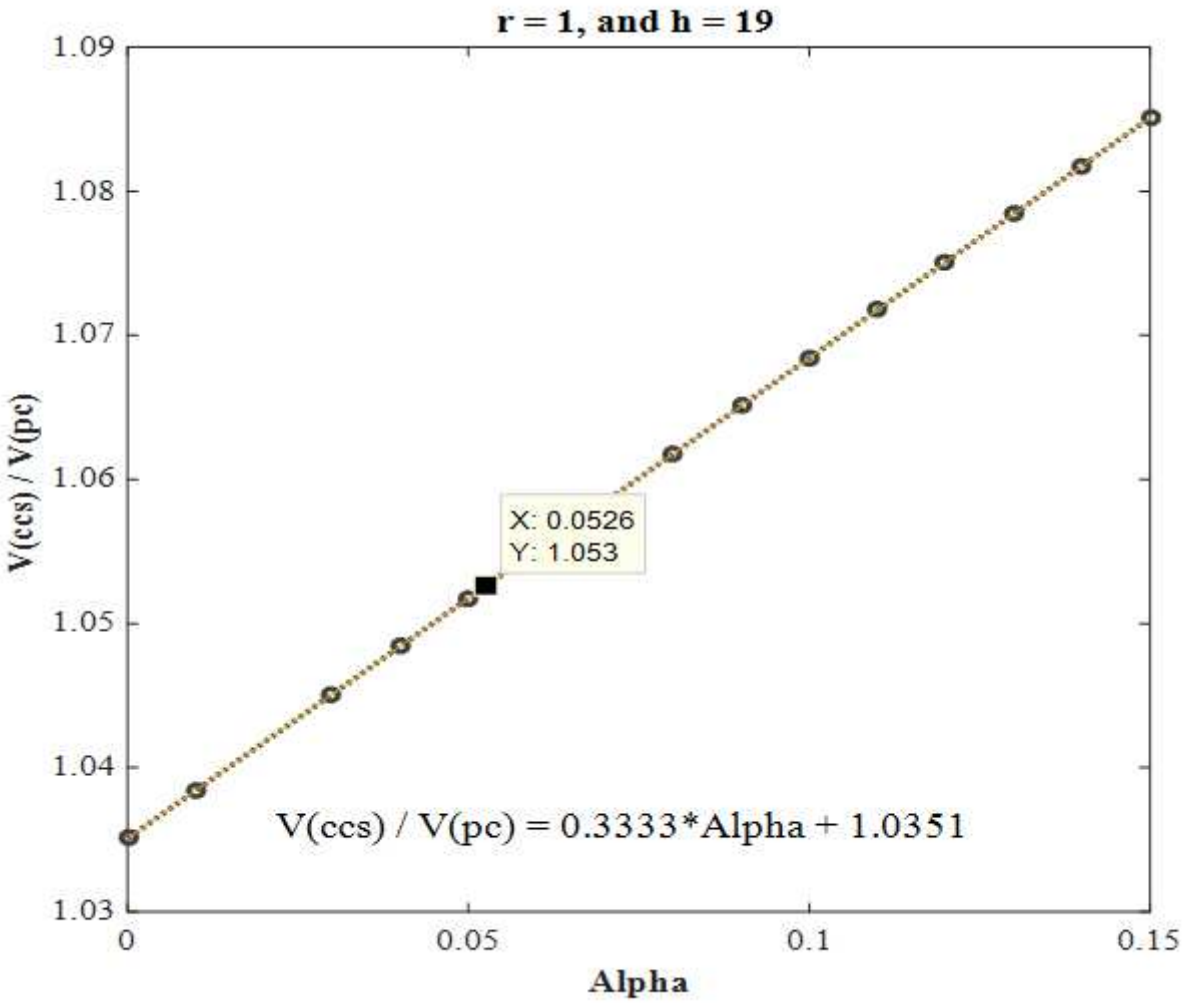

Figure 4

The linear changes of collimator volumetric ratio via the changes of the α parameter at r = 1, and h = 19 mm.

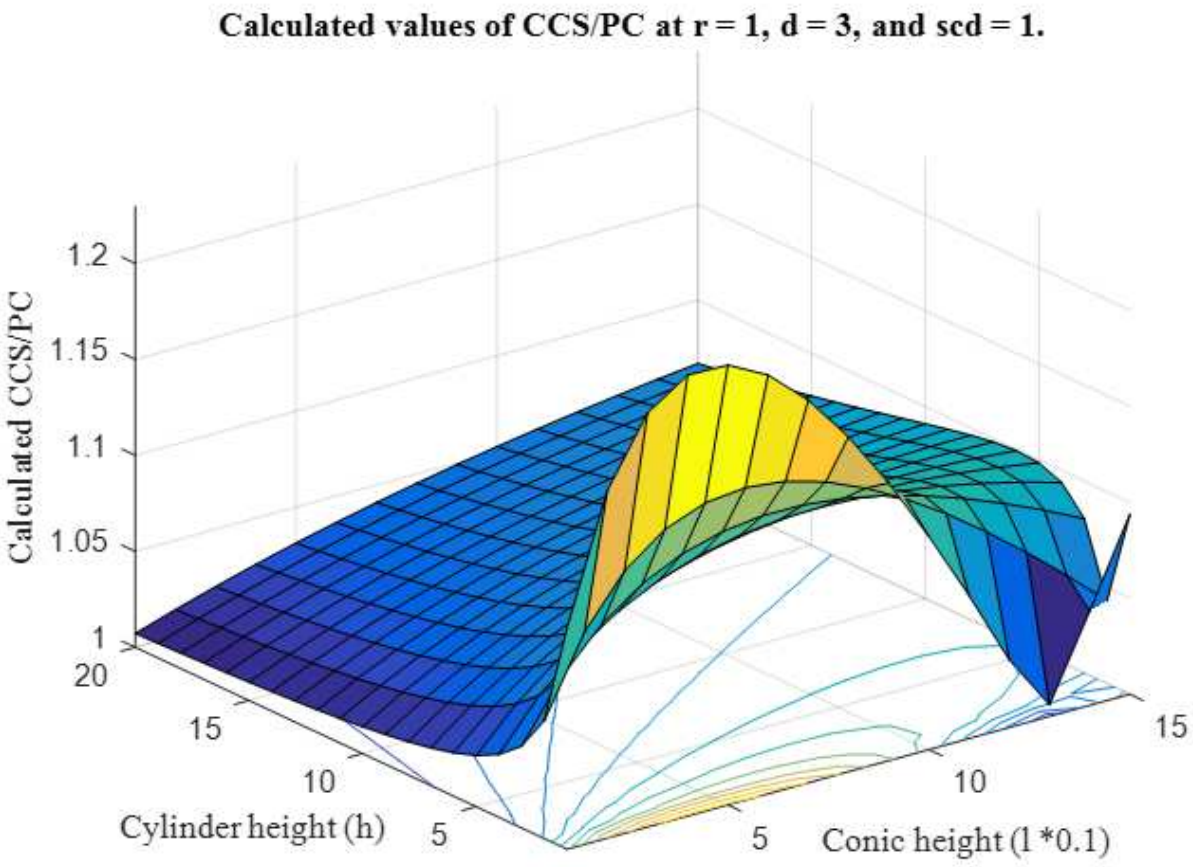

Figure 5

The changes of collimator tracks ratio value against the changes of the cylinder height and the conic height at the r = 1, d = 3, and SCD = 1 mm.

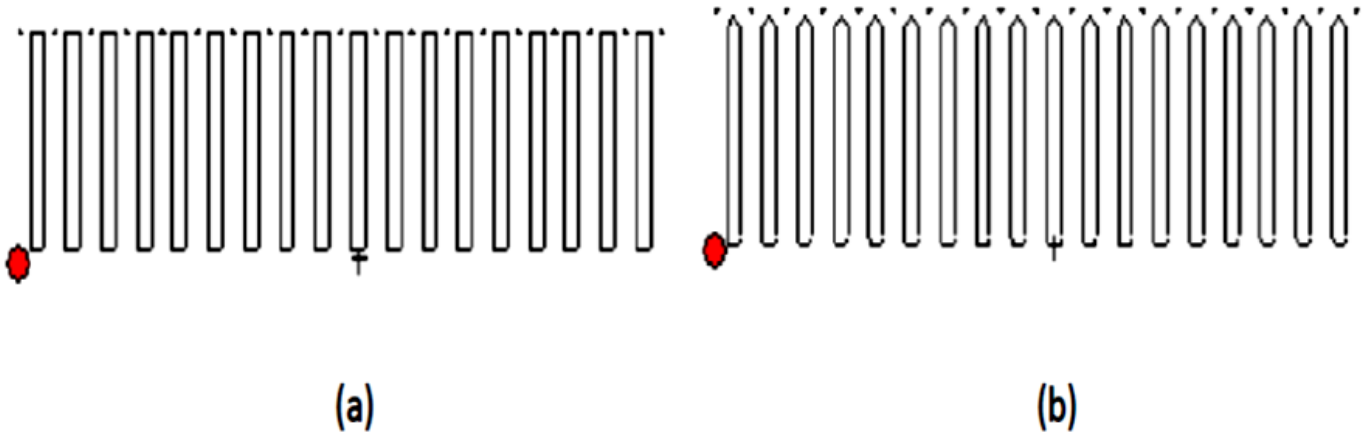

Figure 6

The simulated geometrical results of the configurations by the MCNPX code; (a) the PC, and (b) CCS collimator. The radioactive point sources have been indicated by the red-circle markers, and the point detector is the other side where the F4 tally is calculated.

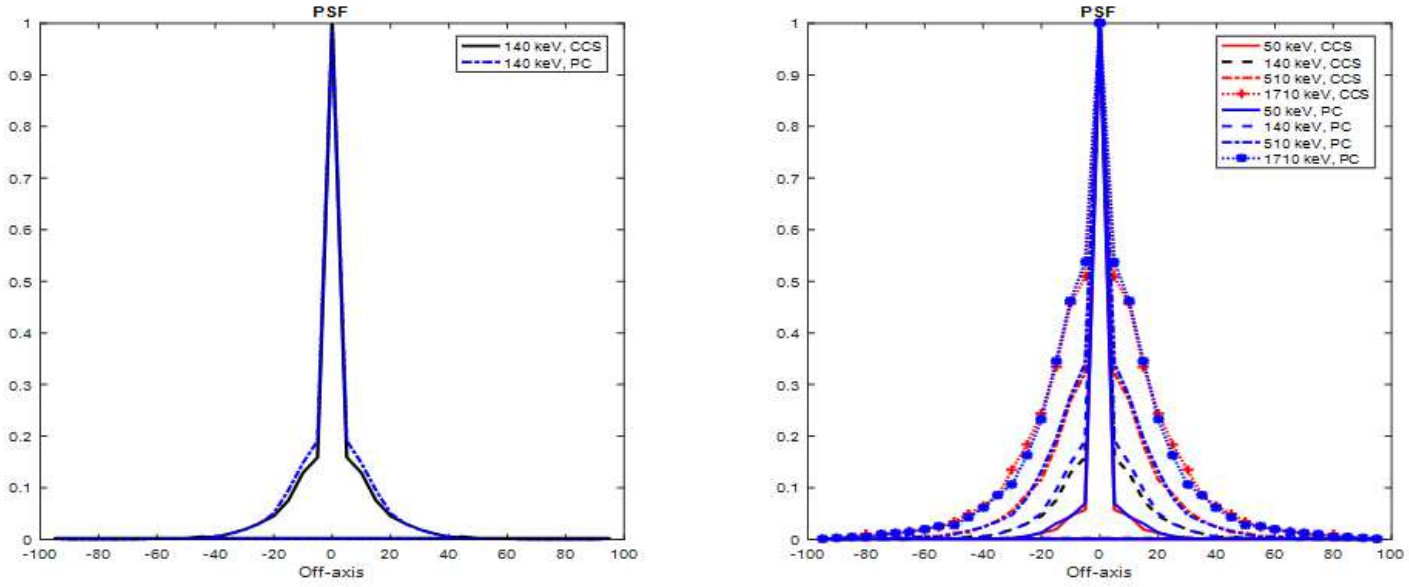

Figure 7

The simulated PSF at the different energies of the source for the PC and CCS collimators.

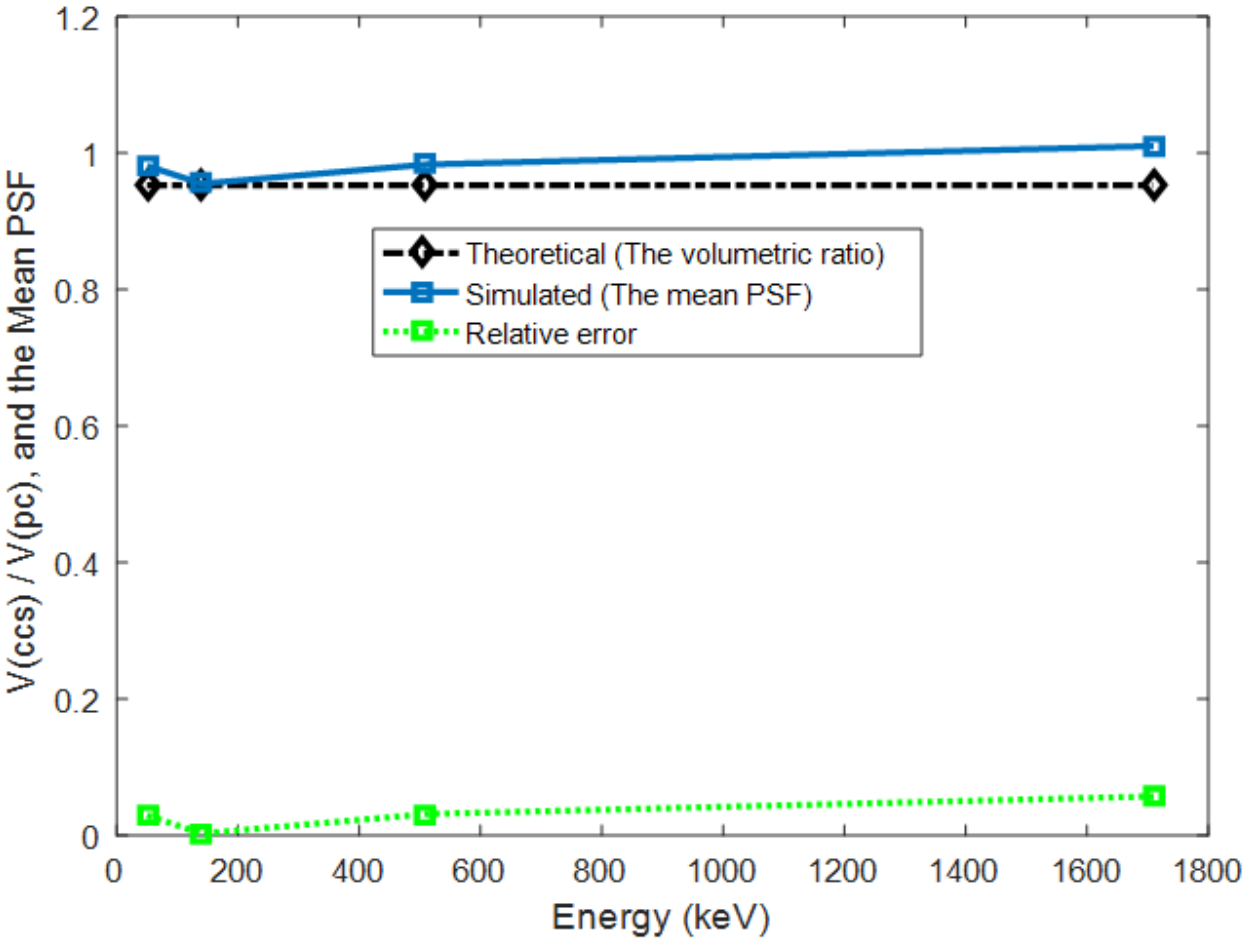

Figure 8

The simulated mean amounts of the PSF and the theoretical-volumetric results via the energy values along with the relative error.

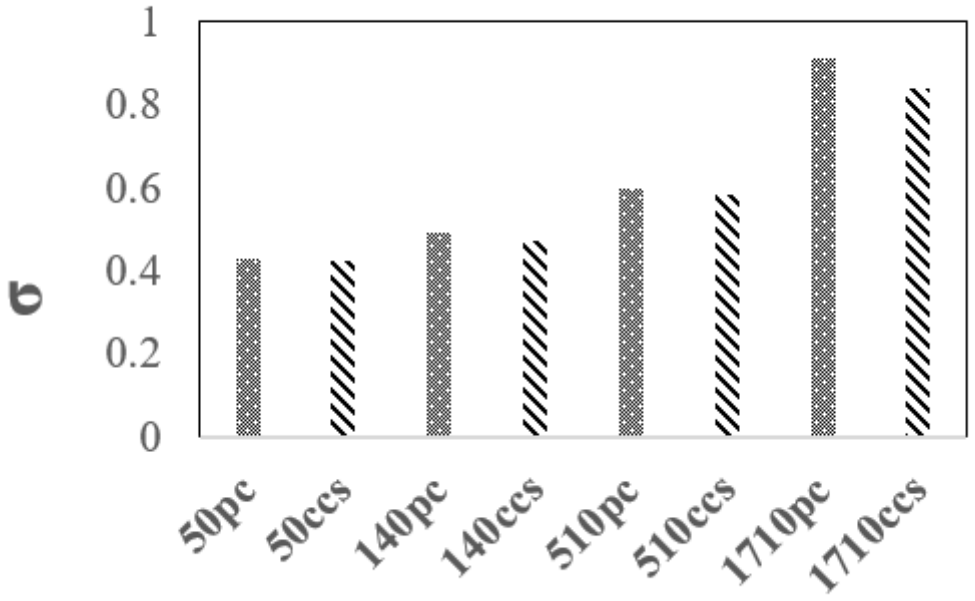

Figure 9

The amounts of the σ parameter for the CCS and PC collimators at the various energies of the source.

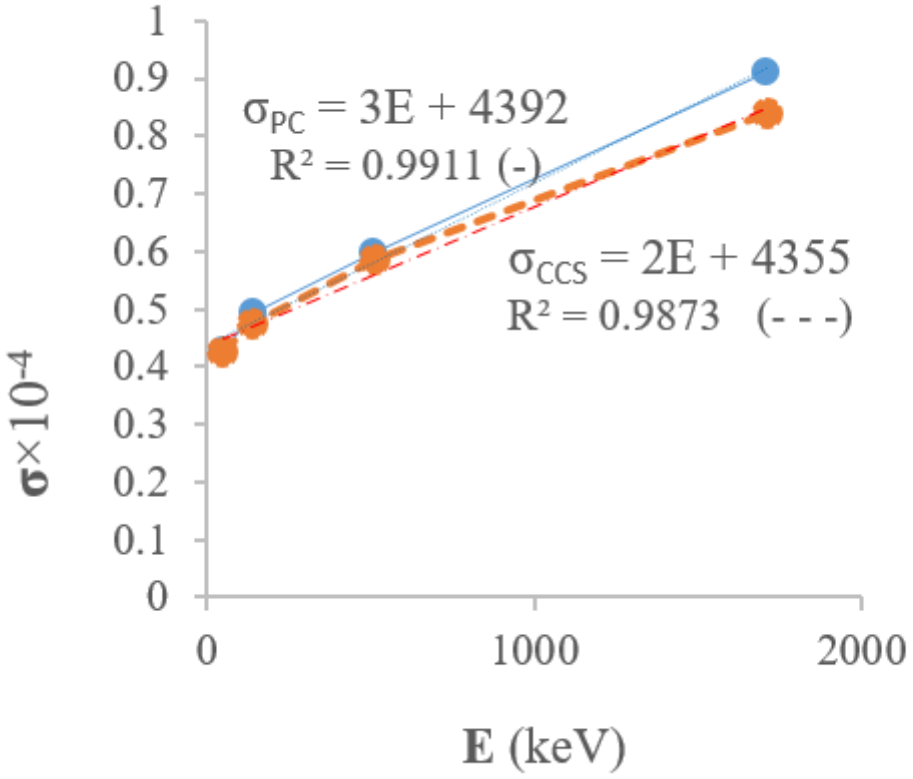

Figure 10

The amounts of the σ parameter in ×10-4 mm at the various energies for the CCS and PC collimators.